Theor Chem Acc (2011) 130:981–990
DOI 10.1007/s00214-011-1039-0

REGULAR ARTICLE

Biradical processes in reactions between benzyne and tropone

Shinichi Yamabe · Tsutomu Minato · Teruyuki Watanabe · Takahisa Machiguchi

Received: 16 August 2010 / Accepted: 3 September 2011 / Published online: 1 October 2011
© Springer-Verlag 2011

Abstract The title reactions were investigated experimentally and theoretically. The benzyne–tropone pair has been known to give a Diels–Alder [4+2] cycloadduct. However, in the present experiment using two sources of benzyne, many unexpected products were obtained. In particular, a zwitterion with a C–Cl bond is strikingly a major product, the structure of which was determined by the X-ray analysis. The bond is formed by quenching the Cl atom from the solvent CH_2Cl_2, which demonstrates that the reactions proceed via radical processes. DFT calculations revealed the elementary processes of the reactions. The presence of the novel zwitterion in the solid state has been interpreted in terms of the permanent dipole–dipole attractions/interactions/stabilization.

Keywords Benzyne · Tropone · Biradical process · Zwitterion · X-ray analysis · DFT calculation

1 Introduction

Benzyne (**1**) is a reactive species [1–6] and is known to work as a dienophile and to give [4+2] cycloadducts in Eq. 1 [7] and Eq. 2 [8].

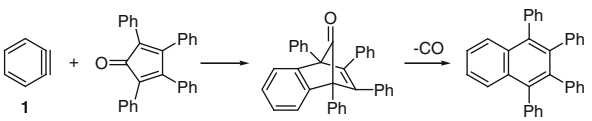

(1)

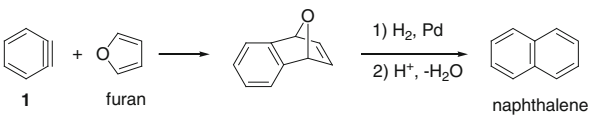

(2)

The species **1** reacts even with an aromatic compound, anthracene, yielding triptycene in Eq. 3 [9].

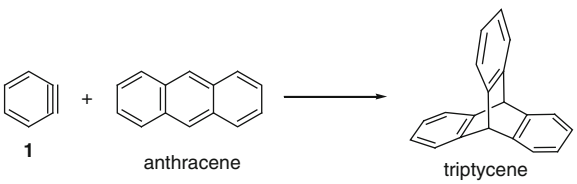

(3)

Thus, **1** has been thought to be a reactive dienophile of Diels–Alder reactions in the normal electron demand [10]. However, the yield of the reaction of **1** with tropone (**2**) is too low (ca. 40%) as a cycloadduct (**6**) in Eq. 4 [11].

Dedicated to Professor Akira Imamura on the occasion of his 77th birthday and published as part of the Imamura Festschrift Issue

Electronic supplementary material The online version of this article (doi:10.1007/s00214-011-1039-0) contains supplementary material, which is available to authorized users.

S. Yamabe (✉)
Department of Chemistry, Nara University of Education, Takabatake-cho, Nara 630-8528, Japan
e-mail: yamabes@nara-edu.ac.jp

T. Minato
Institute for Natural Science, Nara University, 1500 Misasagi-cho, Nara 631-8502, Japan

T. Watanabe · T. Machiguchi
Department of Chemistry, Faculty of Science, Saitama University, 255 Shimo-Ohkubo, Sakura-ku, Saitama 338-8570, Japan

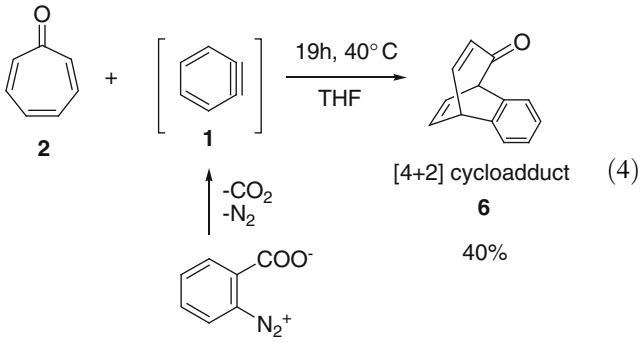

(4)

In addition, the reactions gave a [6+2] cycloadduct as well as a [4+2] one in Eq. 5 [12].

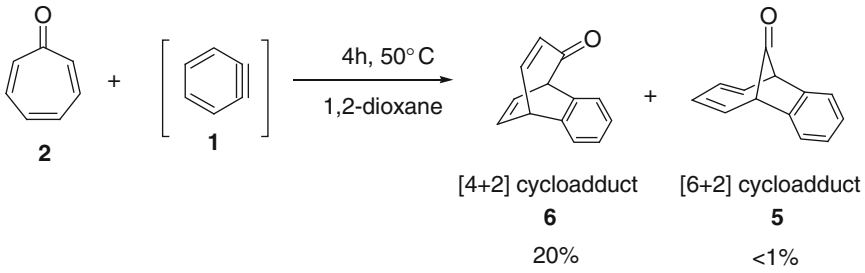

(5)

The species **1** also undergoes a dimerization, i.e., a [2+2] cycloadditon [13]. The "symmetry-forbidden" [14] cycloadducts should arise from stepwise reactions. While zwitterions were suggested in some experimental and theoretical studies [15, 16], recently biradical intermediates were thought to intervene in those symmetry-forbidden reactions [17]. In our previous study [18], a reaction between **1** and tropothione was examined. An anomalous product distribution was explained in terms of the presence of the biradical intermediate. However, the intermediate was not captured experimentally, and its existence is still veiled. Under the confusing status of the benzyne reactivity, we attempted to investigate whether the symmetry-allowed [4+2] reaction in Eq. 4 and symmetry-forbidden [6+2] one in Eq. 5 are concerned with biradical processes.

A doubt on concerted [4+2] cycloadditions of **1** comes from the fact that it does not involve the $sp^2 \rightarrow sp^3$ rehybridization at the dienophile center. Generally, the rehybridization is required to obtain the effective HOMO–LUMO overlapping for the formation of the two C–C bonds. In the [4+2] cycloaddition between benzyne and tropone, the rehybridization in the acetylene of benzyne is infeasible. The deformation (rotation of two olefinic bonds in tropone) is necessary to obtain the effective overlapping as Fig. 1 shows. However, the deformation cannot occur easily because of the seven-membered ring strain. So, the addition path of the benzyne to the tropone may be synchronous but extremely asymmetric. On the other hand, the rehybridization in the olefin and deformation in the butadiene are easy in a typical [4+2] cycloaddition between ethylene and cis-butadiene. Consequently, the [4+2] cycloaddition path is synchronous and symmetric. The [4+2] cycloaddition path is known to be competitive with the one-centered addition path giving a biradical intermediate, as demonstrated in the (ethylene + cis-butadiene) system [19]. Then, the latter path would be more favorable than the former concerted path for the (benzyne + tropone) system.

In this work, definite evidence of the biradical process was found; a chlorine atom of the CH_2Cl_2 solvent is quenched by a reaction intermediate.

2 Experimental results

Benzyne (**1**) was generated in two ways in Eq. 6 [13, 20].

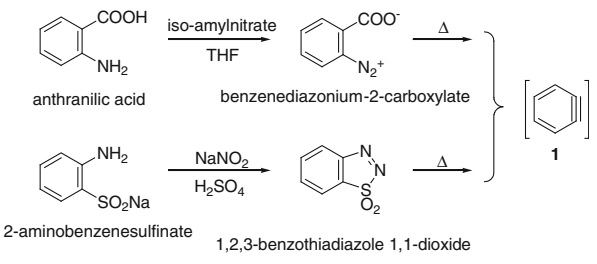

(6)

The reaction between **1** and **2** was performed in CH_2Cl_2 solvent. The products that were obtained are shown in Fig. 2 and exhibit 1:1, 2:1 and 3:1 adducts. The result of the product formation is independent of the benzyne precursor of Eq. 6.

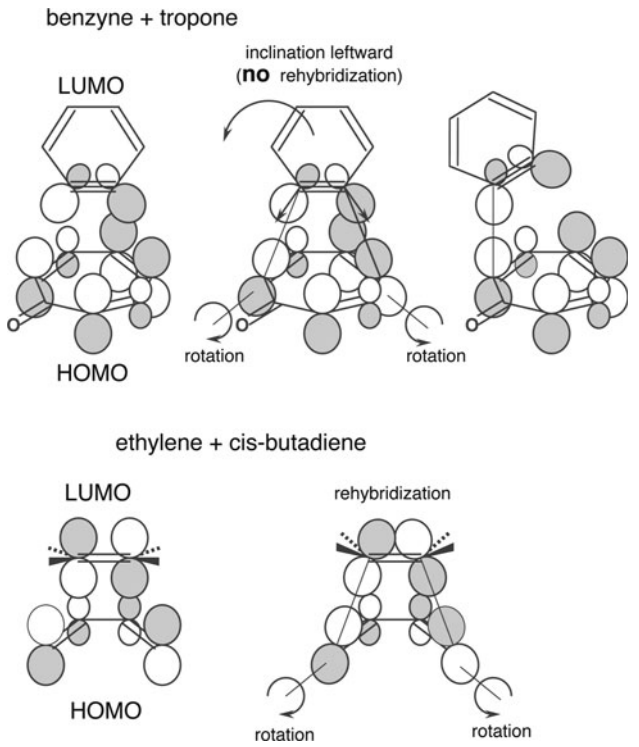

Fig. 1 The schematic presentations of the HOMO–LUMO interaction between benzyne and tropone (*upper*) and that between ethylene and cis-butadiene (*lower*). The *arrows* in the center figure of the (benzyne+tropone) show the direction of the sp^2 hybridization

Although many products were obtained, they are derived primary from the biradical intermediate (**3**), i.e., the one-centered addition product in Eq. 7.

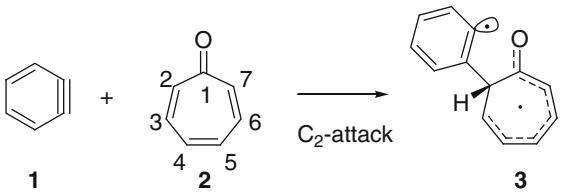

1 **2** **3** (7)

In addition to the cycloaddition, the [4+2] (**6**) and [6+2] (**5**) cycloadducts may be generated by ring closures from **3**. The detailed reaction paths will be explained in the next section. A striking and main product is **15** ([33%]), which has a zwitterion structure. The structure was determined successfully by the X-ray diffraction analysis. The dimer fragment in the accumulated layer of the crystal structure is shown in Fig. 3. The dimer geometry is of point group *i*.

Since the zwitterion form of **15** is very peculiar, an IR measurement of the solid sample of **15** in KBr pellet was made. The obtained frequencies in wave numbers (cm^{-1}) are 3,326 (vs.), 1,914 (w), 1,896 (w), 1,774 (w), 1,592 (s), 1,495 (s), 1,449 (vs.), 1,316 (s), 1,231 (s), 1,153 (m), 1,033 (m) and 746 (vs.). The very strong wave number, 3326 cm^{-1}, may be assigned to the O–H bond stretching vibration. The wave number is close to the BLYP/6-31G(d) value, 3444 cm^{-1} for **15**. This vibrational mode is obviously absent in the neutral geometric isomer, i.e., the ether compound fluorene (**14**). Thus, the solid-state IR data also support the zwitterion structure of **15**.

The product distributions suggest that the (**1**+**2**) reaction proceeds via both the [4+2] cycloaddition and biradical processes. Crucially, the main product **15** has a C–Cl covalent bond, where the source of the chlorine atom is evidently the CH_2Cl_2 solvent. The Cl delivery is feasible only in radical reactions.

3 Computational results and discussions

3.1 The 1:1 adduct intermediates and products

First, the TS of the concerted [4+2] cycloaddition was examined. As expected, the TS geometry is highly asymmetric and is shown in Figure S2. One newly forming C–C bond distance is 2.532 Å, and the other one is 3.085 Å. The high asymmetry is consistent with the discussion based on the HOMO–LUMO interactions in Fig. 1.

Second, the one-centered addition was examined. The addition TS, TS (**1**+**2** → **3**) and the consequent biradical adduct **3** were obtained. Their geometries are shown in Figure S3. The TS geometry is as if it were for the [8+2] cycloaddition. That is, at the C···O region (3.308 Å), the secondary orbital interaction is operative. Superiority or inferiority of [4+2] path (Figure S2) and the one-centered path (Figure S3) were examined. Their activation energies are similar (3.7 kcal/mol for the one-centered path and 4.0 kcal/mol for the [4+2] path), and the activation entropies are also similar (−39.1 kcal/K/mol and −39.5 kcal/K/mol). Therefore, both reactions are expected. The one-centered addition is slightly more favorable than the [4+2] cycloaddition.

Isomerization processes from **3** were sought, and the obtained products are shown in Fig. 4.

Transition-state and related geometries are shown in Figure S5.

The benzyne ring can rotate almost freely around the newly formed C–C bond. The intermediate **3** gives four cycloadducts, **4**, **5**, **6** and **7**. The electronic reaction energies with zero-point correction (relative to that of **1** + **2**) are −72.2 (**4**), −73.9 (**5**), −75.9 (**6**) and −53.2 kcal/mol (**7**). Among the four cycloadducts, the cyclobutane **7** is significantly unstable and is unlikely. While **5** and **6** have been obtained in the present experiment, the [8+2] cycloadduct **4** has not been detected. This species would undergo some subsequent radical reactions, which will be discussed in the Sect. 3.4. For the reaction with the molar ratio [**1**]:[**2**] = 1:1, the major product is the [4+2]

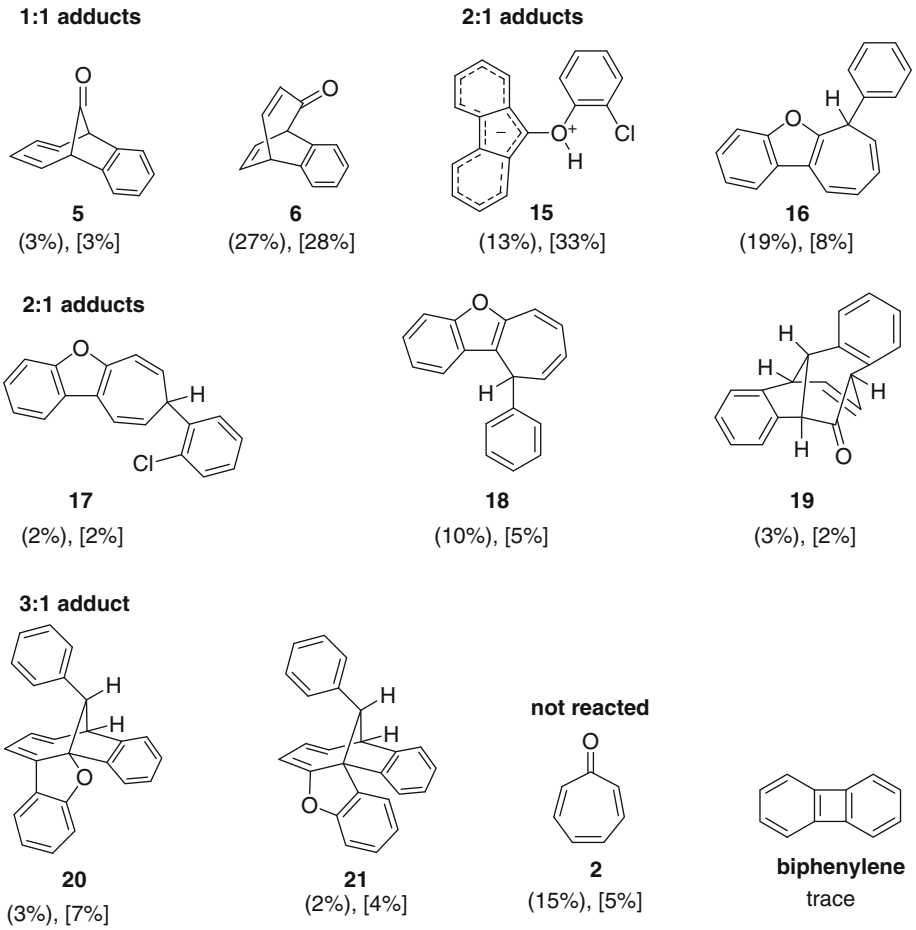

Fig. 2 Summary of the products obtained in the present experiment. The precursor is benzenediazonium-2-carboxylate in Eq. 6. Yields in parentheses are by the reaction of the molar ratio, [**1**]:[**2**] = 1:1 (Figure S4a in Supporting Information). Those in the *square brackets* are with [**1**]:[**2**] = 2:1 (Figure S4b in Supporting Information)

cycloadduct (**6**), 27%, as shown in Fig. 2. This adduct may be afforded both by the concerted addition, TS(**1** + **2** →**6**), and by the isomerization from **3**. Therefore, the difference in the yields of the two 1:1 adducts (3%) of **5** and (27%) of **6** suggests that the [4+2] adduct is derived from the two routes. This is because **5** and **6** may be produced almost equally from **3** via the rotation ring closure. The similar yields, (27%) and [28%], of **6** indicate that the [4+2] cycloadduct is generated solely by bimolecular (**1**+**2**), not termolecular reactions.

3.2 The 2:1 adduct intermediates

In Fig. 2, various 2:1 adducts have been present. Among them, the zwitterion **15** is the major product. Its formation path was traced. The biradical **3** may be subject to addition of the second benzyne. The exo-cyclic oxygen is less sterically crowded than the carbon radical centers and may be combined with **1**, which leads to the biradical **8** (Fig. 5). Hereafter, reaction paths were sought in the criterion of extension of conjugated moieties including the formation of benzene ring and retention of the radical character as much as possible.

The paths shown by the dotted arrows were not traced. The detailed computed data of TS(**1** + **2** → **3**), TS(**8** + CH_2Cl_2 → **9**$^{\cdot}$ + $CH_2Cl^{\cdot}$), TS(**9**→**10**), TS(**10** → **11**), TS(**11**→**12**) and TS(**12** → **13**) are in Supporting Information. Alternative paths for **12** → **14** are depicted, which includes **14**a, **14**b, **14**c and **14**d in the consecutive H [1,5] sigmatropic shifts.

The species **8** has two in-plane sp^2 radical lobes. One (new) lobe is surrounded more by solvent (CH_2Cl_2) molecules than the other. Here, a striking reaction occurs; the solvent Cl–C bond is cleaved by the former lobe, TS (**8** + CH_2Cl_2 → **9**$^{\cdot}$ + $CH_2Cl^{\cdot}$), shown in Fig. 6.

A doublet radical **9** is formed. Further processes need to be directed for conversion of the seven-membered ring of **9** to the benzene ring in view of the structure of **15**. For the conversion, the radical center in **9** is connected to the α carbon of the seven-membered ring, TS (**9** → **10**). A cyclobutane **10** is afforded. The ring strain of the cyclobutane ring is large, and one C–C bond is long (=1.603 Å). Its scission gives a nine-membered radical **11** via TS (**10** → **11**). The radical is transformed to **12** of the six-membered ring through TS (**11** → **12**). Next, the H [1,2] shift TS, TS (**12** → **13**), was obtained. Energy changes

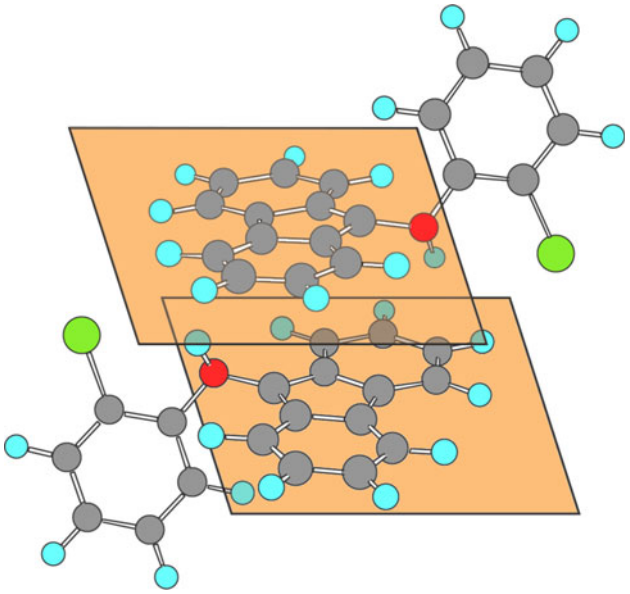

Fig. 3 The geometry of the dimer unit (**15**+**15**) in the crystal. *Gray*, *light blue*, *red* and *olive color circles* denote carbon, hydrogen, oxygen and chlorine atoms, respectively. The crystal structure was determined by the present X-ray analysis. The detailed geometric data are shown in Figure S1 (Supporting Information)

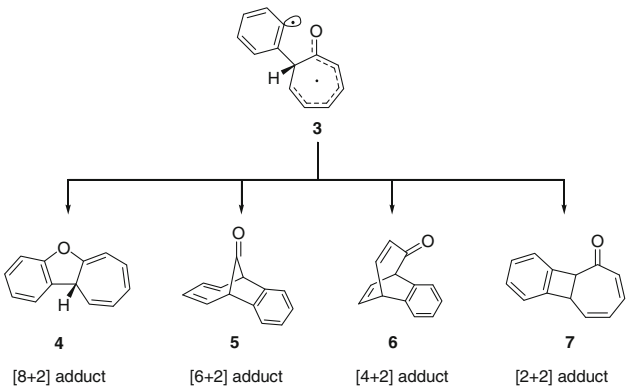

Fig. 4 Four cycloadducts produced from the biradical intermediate **3**

along the path, **9** → **10** → **11** → **12** → **13**, are exhibited in Table 1. The resultant doublet radical (**13**) has a long C–H bond (1.113 Å). The bond may be cleaved readily by attack of another benzyne. In fact, in the (**13** + benzyne) system, partial optimizations with the fixed and assumed C–H distances give monotonic energy descent. Therefore, the H abstraction TS could not be obtained. That is, the step, **13** → **14** + H$^{\cdot}$, is quite probable. Alternatively, the hydrogen atom in **13** may be quenched by the $CH_2Cl^{\cdot}$ radical formed at **8** → **9**. A 9-O-aryl-substituted fluorene **14** is arrived at. The tricyclic aromatic hydrocarbon **14** is a stable compound and appears to be the obtainable product. However, the product of the solid state detected in the previous section is the zwitterion **15** (Fig. 3). Formally, the ion **15** is generated from the fluorene **14** via H [1,2] shift. However, the isomerization from the stable fluorene seems to be unlikely. There should be another factor to cause the (**14**→**15**) conversion, and we take that up in the next section.

By the use of dimer, trimer and tetramer fragments in the crystal structure of **15**, their geometry optimizations were carried out. The obtain results are displayed in Table 2. Isomers of **14**c and **14**d are involved in the optimized geometries. Their structural formulae are shown in Fig. 5. Figure S9 shows that the **14**d dimer form was obtained starting from the **15** one of the crystal moiety. The optimization of $(\mathbf{15})_4$ leads alternatively to a system composed of $(\mathbf{14}c)_2$ and $(\mathbf{14}d)_2$ (Table 2). Thus, the route up to the zwitterion **15** is thought to be via the intermediates **14**c and **14**d. These species are derived from **14**b and **14**a, respectively, via H[1,5] shifts (Fig. 5).

3.3 Formation of a zwitterion in the crystal structure

The following figure shows structural formulae of the fluorene **14** and the zwitterion **15**.

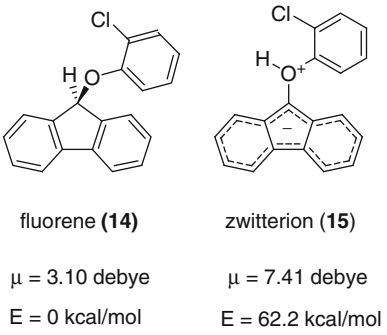

The ion **15** is by 62.2 kcal/mol unstable relative to **14**. On the other hand, the zwitterion **15** is a polar species and its dipole moment was calculated to be 7.41 debye, while that of the fluorene **14**, 3.10 debye. The former value may cause a permanent dipole–dipole attraction in the anti-parallel orientation (Fig. 7).

The way of calculating the attraction energy is explained in Sect. 5.3. The 4.061 Å distance between two molecular planes in the crystal structure of Fig. 3 is approximated by 4.0 Å for calculating the attraction energy.

The attraction (stabilizing) energy of (**15** + **15**) was calculated to be −170 kcal/mol, while that of (**14** + **14**), −5.2 kcal/mol (See Sect. 5.3 Calculation of dipole–dipole attraction energies). This energy difference overcomes that of the above-mentioned unimolecular energy difference, i.e., 2 × 62.2 kcal/mol < (170–5.2) kcal/mol. In fact, the dimer unit in the crystal structure (Fig. 3) has the anti-parallel orientation in the point group *i*. Thus, the zwitterion **15** can be present only as accumulated and stacked

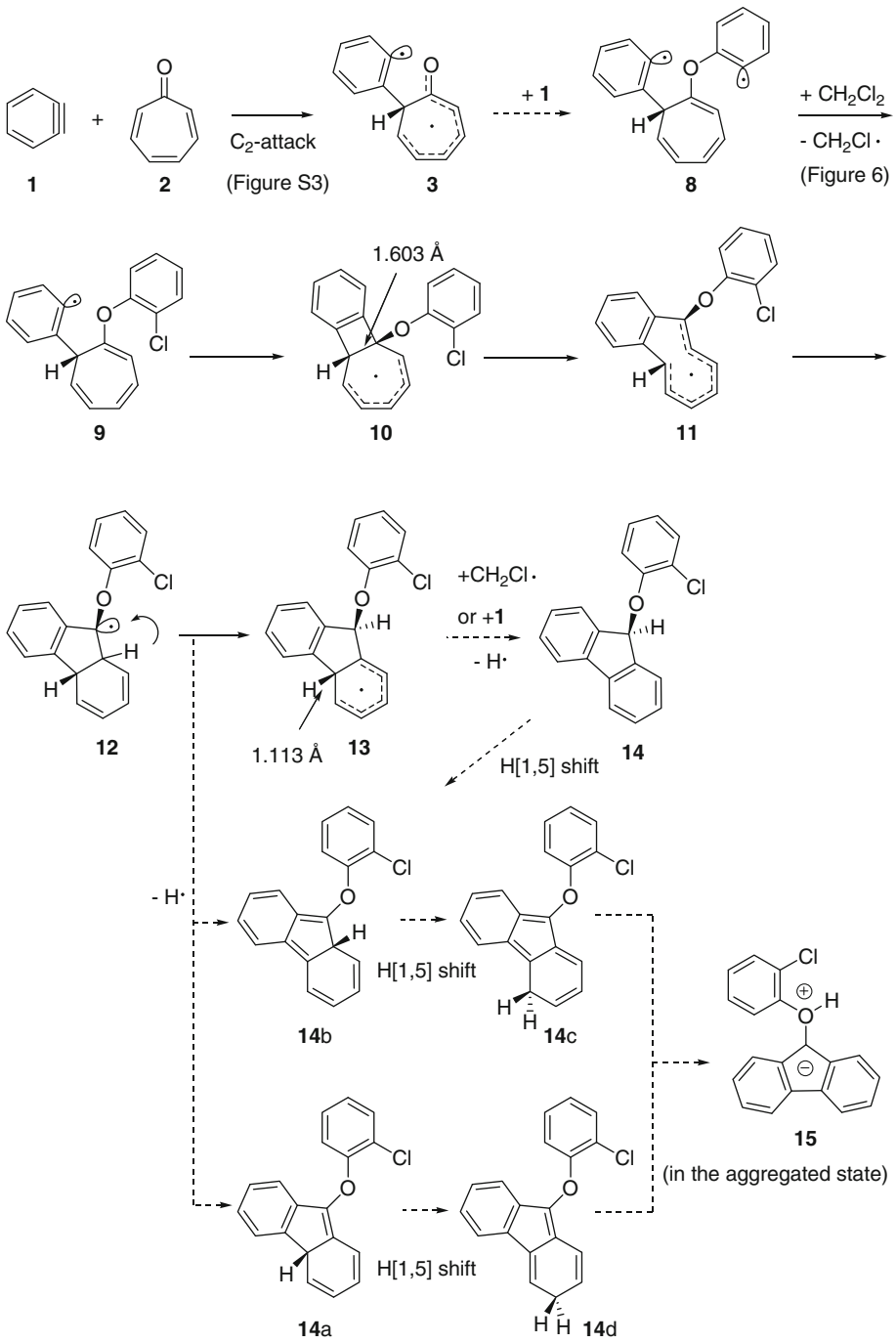

Fig. 5 The calculated reaction paths toward the major product, **15**

aggregates in the anti-parallel form. The isomerization, **14** → **15**, is thought to occur by the intermolecular mutual proton transfer during the crystal growth. Once the crystal is dissolved in the solvent (e.g., CH_2Cl_2), the ion form **15** is instantly converted to the fluorene **14** via the mutual proton transfer. In fact, when the geometry of the dimer of **15** in Fig. 3 is optimized, it becomes that of **14**c + **14**d or **14**d + **14**d. These species are shown in Fig. 5. Table 2 shows various geometries of the dimer and those of the trimer and tetramer. They were optimized starting from that of the dimer of **15** shown in Fig. 3. Three dimer geometries of (**14**d + **14**d), (**14**c + **14**d) and (**15** + **15**) are shown in Figures S9, S10 and S11, respectively.

Recently, we detected a zwitterion in a ketene–olefin reaction spectroscopically [21]. Its presence was interpreted in terms of the permanent dipole–dipole attraction. According to the interpretation, a dimer of the zwitterion in the anti-parallel combined conformation was monitored

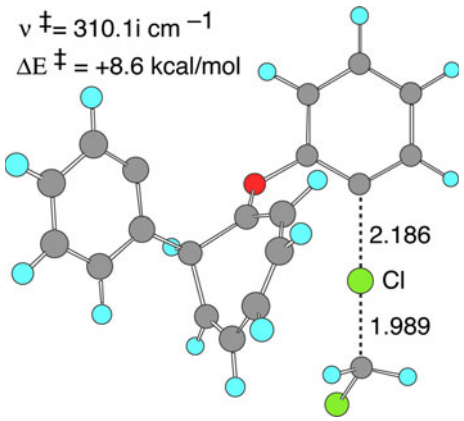

Fig. 6 The geometry of TS (**8** + CH_2Cl_2 → **9**˙ + CH_2Cl˙). *Gray*, *light blue*, *red* and *olive color circles* denote carbon, hydrogen, oxygen and chlorine atoms, respectively. Distances are in angstrom. $\nu^{\ddagger}$ stands for the sole imaginary frequency. $\Delta E^{\ddagger}$ is the activation energy relative to the sum of the **8** and CH_2Cl_2 energies

Table 1 Relative Energies Starting from **9** (=0) to **13**

	Relative energy (kcal/mol)	
	ΔE	ΔG
9	0 (0)	0
TS (9→10)	8.8 (8.8)	9.3
10	−17.1 (−18.1)	−15.8
TS (10→11)	13.6 (12.8)	14.9
11	−6.1 (−6.7)	−5.0
TS (11→12)	3.7 (2.7)	4.9
12	−30.7 (−30.8)	−29.4
TS (12→13)	−5.1 (−5.1)	−3.7
13	−42.6 (−43.4)	−41.3

ΔE and ΔG stand for the relative electronic energy (with zero-point corrections) and relative Gibbs free energy (T = 298K, P = 1atm), respectively. The values in parentheses are the relative energies including the SCRF = PCM solvent effect (solvent is dichloromethane)

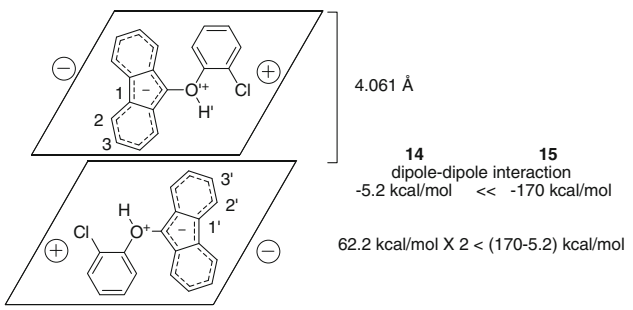

Fig. 7 The anti-parallel-oriented dimer which gives the large permanent dipole–dipole attraction

successfully. Even if the monomers are unstable, formation of the anti-parallel array of the polar species gives rise to the aggregation.

3.4 Formation of the other 2:1 adducts than **15**

Figure 2 has shown other 2:1 adducts than **15**. Formation of the other adducts is discussed here. The [8+2] adduct **4** is only slightly less stable than [6+2] (**5**) and [4+2] (**6**) adducts. However, **4** is not obtained in the present experiment. The bridge-head C–H bond is long (=1.107 Å), and the hydrogen would be abstracted readily by some radical species, e.g., CH_2Cl˙ (Fig. 8). When the hydrogen is removed, a 3-furyl radical (**4**-H, **4** minus H˙) is produced. The furyl moiety isomerizes to a furan moiety to form the 6π-electron system. Thus, in the radical with a furan structure, three canonical resonance structures, (**4**-H)a, (**4**-H)b and (**4**-H)c, coexist. Each may be linked with the other benzyne (**1**). Then, the added benzyne moiety is converted to the phenyl or aryl ring in the products, **16**, **17** and **18** (Fig. 2).

The [8+2] cycloadduct **4** may undergo the H˙ abstraction, which is similar to the (**13** → **14**) step in Fig. 5. Subsequently, the resultant radical (**4**-H) may be combined with the second benzyne.

4 Concluding remarks

In this work, the benzyne–tropone reaction was studied experimentally and computationally. In addition to the reported 1:1 adducts of [4+2] (**6**) and [6+2] (**5**), we obtained a novel 2:1 adduct (**15**) as a main product. Their formation is initiated by a biradical intermediate **3** (Fig. 9). The biradical character was elucidated for the first time by the Cl quench from the solvent CH_2Cl_2.

Indeed, the zwitterion **15** appears to be unstable compared to the neutral isomer, fluorene **14**, but the permanent dipole–dipole interaction brings about the stability of **15** in the crystal structure. Noteworthy is that the crystal structure of the zwitterion could not be obtained when the CH_2Br_2 solvent is used instead of CH_2Cl_2. The fluorene **14**(Br) is the product. The failure of formation of the zwitterion **15**(Br) comes from the difficulty in the anti-parallel orientation of the two ions by the large-size bromine substituents (see Figure S8). Examination of the correlation between the zwitterion formation and the size of substituents is now in progress.

By nature, the benzyne **2** has two in-plane sp^2 hybridized orbitals. Its rigid directionality of the angle 120° degree cannot conform to the (sp^2 → sp^3) rehybridization at cycloadditions. The benzyne works as a biradical reagent along with as a dienophile toward conjugated compounds.

Table 2 Various geometries of dimer and those of trimer and tetramer

Method Basis set	Crystal	Dimer BPW91(SCRF) 6-311+G(d,p)	Dimer[a] BPW91(SCRF) 6-311+G(d,p)	Dimer MP2 6-31G(d)	Dimer BPW91 6-31G(d)	Trimer BPW91 6-31G(d)	Tetramer[b] BPW91 6-31G(d)
H–C2	2.504	2.136	8.284	1.103	2.143	1.111	1.111 (1.111)
H–C3	3.286	1.109	8.255	2.130	1.111	2.128	2.122 (2.123)
H′–C2′	2.664	2.140	8.417	2.116	2.144	2.146	2.145 (2.146)
H′–C3′	2.504	1.109	8.269	1.100	1.112	1.112	1.112 (1.112)
O–H	0.992	3.518	0.994	2.630	3.232	3.483	3.127 (3.325)
O–H′	0.992	4.667	0.994	2.687	4.796	11.540	5.698 (6.446)
Result		**14**d, **14**d	**15**, **15**	**14**c, **14**d	**14**d, **14**d	**14**c, **14**d, **15**	**14**c*2, **14**d*2

H, H′, C2′, C2′, C3 and C3' are defined in Fig. 7. Bond distances are shown in Å. In the "result" item, the obtained fragment geometries (**14**c, **14**d and **15**) are exhibited. Their structural formulae are displayed in Fig. 5

[a] Another dimer in crystal, hydronium hydrogens toward the outside of the dimer. (Figure S11)

[b] A tetramer is composed of two dimers. The geometric parameters of one dimer are shown in parentheses

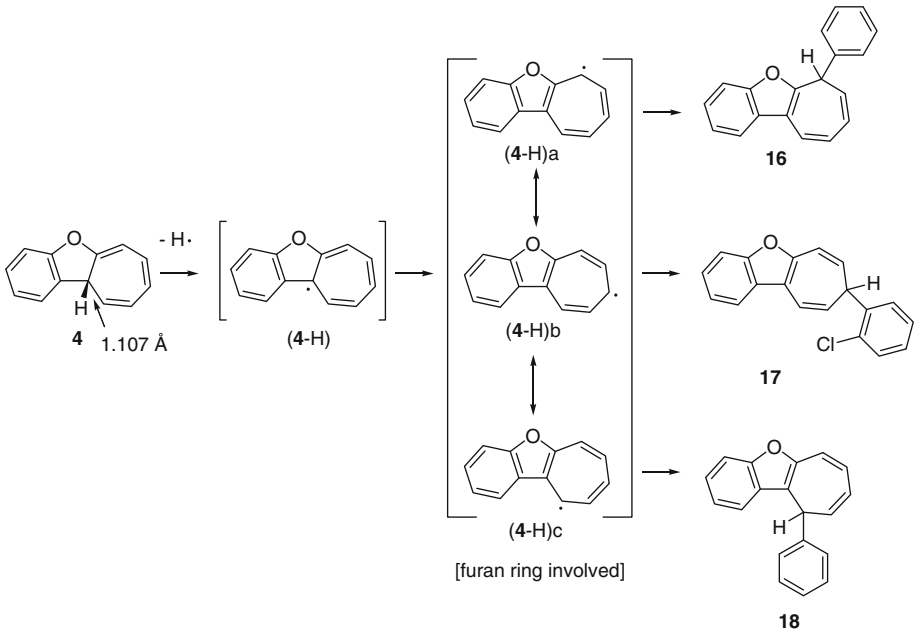

Fig. 8 Further reactions of [8+2] product (**4**)

5 Methods and results of experiment and methods of computation

5.1 Experimental method and results

Typical experimental procedure.

(1) The reaction of the molar ratio [**1**]/[**2**] = 1.

Mixtures of dichloromethane (23 mL), tropone (**2**, 0.71g, 6.70 mmol) and benzenediazonium-2-carboxylate prepared from anthranilic acid (1.00 g, 7.28 mmol) and iso-amyl nitrate (1.39 g, 11.9 mmol) were heated at 40 °C under nitrogen reflux. The reaction was monitored by HPLC. For HPLC, the small and settled amount of the solution was taken periodically, cooled in the ice bath, and washed with water. After 5% $NaHCO_3$ was added to the solution, it was adjusted to pH = 7.0. It was dried by magnesium sulfate and concentrated.

(2) The reaction of the molar ratio [**1**]/[**2**] = 2.

Mixtures of dichloromethane (23 mL), tropone (**2**, 0.72 g, 6.80 mmol) and benzenediazonium-2-carboxylate prepared from anthranilic acid (1.99 g, 14.5 mmol) and iso-amyl nitrate (2.79 g, 23.8 mmol) were heated at 40 °C under nitrogen reflux. Then, the same procedure as in (1) was taken for the HPLC analysis.

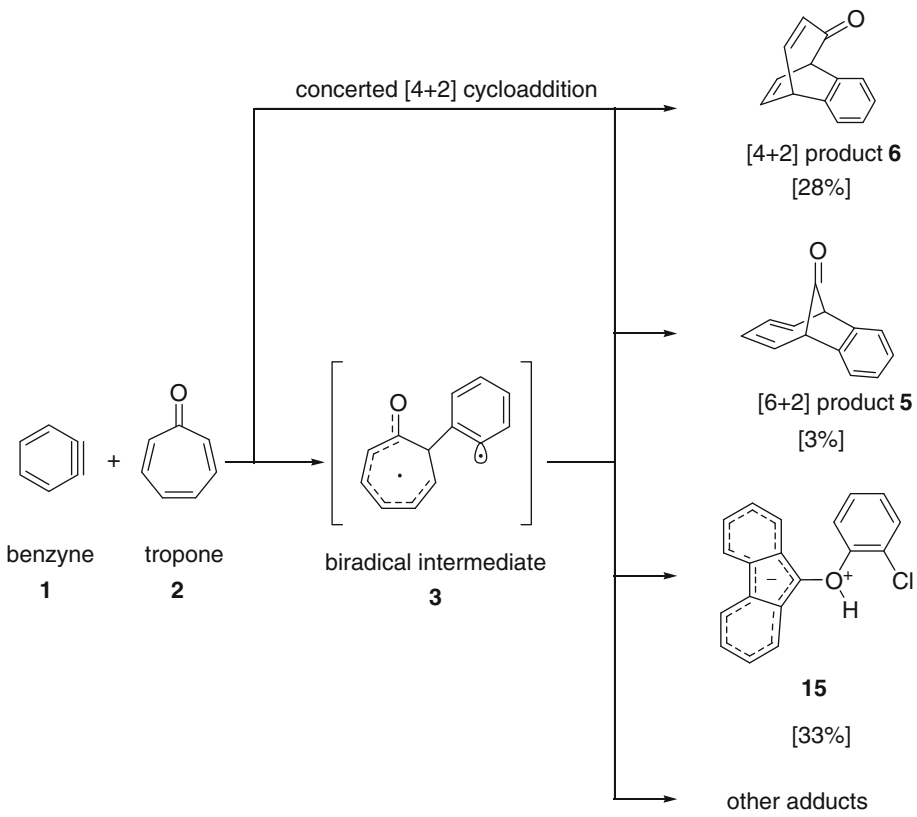

Fig. 9 Summary of the present study. Yields (%) are from the reactant molar ratio, [**1**]:[**2**] = 2:1

5.2 Computational method

The BPW91 DFT method was used for the geometry optimizations. It is composed of the Becke88 gradient-corrected exchange-energy functional with the proper asymptotic limit [22] and the Perdew/Wang 91 gradient-corrected correlation-enery functional [23]. BPW91 has been frequently applied to radical and biradical species [24–26]. Also, the electronic structure of the benzyne was examined by BPW91 [27]. Other DFT calculations, B3PW91 [28–33], M05 [34, 35] and M06 [36], were carried out. Symmetry-broken singlet biradical orbital is formed by mixing of HOMO and LUMO. The basis set used was 6-311+G(d,p). Transition states were verified by sole imaginary frequencies. Relative energies with SCRF = PCM [37–39] were calculated and are shown in Table 1. All the calculations were carried out, using GAUSSIAN03 program package [40], which is installed at the Research Center for Computational Science, Okazaki Japan.

5.3 Calculation of dipole–dipole attraction energies

Definition of dipole–dipole interaction is shown in Eq. 8 [41].

$$U_{d-d}(r) = -\frac{2 \times \mu_1^2 \times \mu_2^2}{(4\pi\varepsilon_0)^2 \times 3 \times k_B \times T} \times \frac{1}{r^6} \tag{8}$$

r: distance; μ_1, μ_2: values of the dipole moments; At T = 300 K; $4\pi\varepsilon_0$ = 1.11265×10^{-10} $C^2\ J^{-1}\ m^{-1}$; k_B = 1.380658×10^{-23} $J\ K^{-1}$ (Boltzmann constant); 1 debye = 3.3356×10^{-30} Cm.

(1) fluorene (**14**); r: 4.0 Å shown in Fig. 7. μ_1, μ_2: 3.10 debye.

$$\begin{aligned} U_{d-d}(4.0) &= -\frac{2 \times (3.10 \times 3.3356 \times 10^{-30})^4}{(1.112666 \times 10^{-10})^2 \times 3 \times 1.380658 \times 10^{-23} \times 300 \times (4.0 \times 10^{-10})^6}\,\mathrm{J} \\ &= -3.6288 \times 10^{-20}\,\mathrm{J} \\ &= -5.23\,\mathrm{kcal/mol} \end{aligned}$$

(2) zwitterion (**15**).
r : 4.0 Å shown in Fig. 7. μ_1, μ_2 : 7.41 debye.

$$U_{d-d}(4.0) = -\frac{2 \times (7.41 \times 3.3356 \times 10^{-30})^4}{(1.11265 \times 10^{-10})^2 \times 3 \times 1.380658 \times 10^{-23} \times 300 \times (4.0 \times 10^{-10})^6}\,\mathrm{J}$$
$$= -1.18466 \times 10^{-18}\,\mathrm{J}$$
$$= -170.6\,\mathrm{kcal/mol}.$$

Acknowledgments We thank five reviewers for their careful examinations and fruitful comments.

References

1. Roberts JD, Simmons HE, Carismith LA, Vaughan CW (1953) J Am Chem Soc 75:3290–3291
2. Washburn WN (1975) J Am Chem Soc 98:1615–1616
3. Washburn WN, Zahler R (1976) J Am Chem Soc 98:7827–7828
4. Washburn WN, Zahler R (1976) J Am Chem Soc 98:7828–7830
5. Jones RR, Bergman RG (1972) J Am Chem Soc 94:660–661
6. Breslow R, Napierski J, Clarke TC (1975) J Am Chem Soc 97:6275–6276
7. Fieser LF, Haddadin M J (1966) Org Synth 46: 107. http://www.orgsyn.org/orgsyn/pdfs/CV5P1037.pdf
8. Wittig G, Pohmer L (1955) Angew Chem 67:348
9. Friedman L, Logullo FM (1969) J Org Chem 34:3089
10. Sustmann R, Schubert R (1972) Angew Chem Int Ed 11:840
11. Ciabattoni J, Crowley JE, Kende AS (1967) J Am Chem Soc 89:2778
12. Miwa T, Kato M, Tamao T (1969) Tetrahedron Lett 22:1761
13. Logullo FM, Seitz AH, Friedman L (1968) Org Synth 48:12. http://www.orgsyn.org/orgsyn/pdfs/CV5P0054.pdf
14. Woodward RB, Hoffmann R (1970) The conservation of orbital symmetry. Verlag Chemie, New York
15. Wasserman HH, Solodar AJ, Keller LS (1968) Tetrahedron Lett 21:5597
16. Hayes DM, Hoffmann R (1972) J Phys Chem 76:656
17. Ozkan I, Kinal A (2004) J Org Chem 69:5390
18. Yamabe S, Minato T, Ishiwata A, Irinamihira O, Machiguchi T (2007) J Org Chem 72:2832–2841
19. Goldstein E, Beno B, Houk KN (1996) J Am Chem Soc 118:6036–6043
20. Wittig G, Hoffmann RW (1967) Org Synth 47: 4. http://www.orgsyn.org/orgsyn/pdfs/CV5P0060.pdf
21. Machiguchi T, Okamoto J, Morita Y, Hasegawa T, Yamabe S, Minato T (2006) J Am Chem Soc 128:44–45
22. Becke AD (1988) Phys Rev A 38:3098
23. Perdew JP, Wang Y (1992) Phys Rev B 45:13244
24. Tichy SE, Nelson ED, Amegayibor FS, Kenttamaa HI (2004) J Am Chem Soc 126:12957–12967
25. Littleford RE, Paterson MAJ, Low PJ, Tackley DR, Jayes L, Dent G, Cherryman JC, Brown B, Smith WE (2004) Phys Chem Chem Phys 6:3257–3263
26. Tripathi GNR, Chipman DM (2002) J Phys Chem A 106: 8908–8916
27. Cremer CJ, Nash JJ, Squires RR (1997) Chem Phys Letters 277:311
28. Becke AD (1993) J Chem Phys 98:5648
29. Burke K, Perdew JP, Wang Y (1998) In: Dobson JF, Vignale G, Das MP (eds) Electronic density functional theory: recent progress and new directions. Plenum, Berlin
30. Perdew JP (1991) In: Ziesche P, Eschrig H (eds) Electronic Structure of Solids'91. Akademie Verlag, Berlin, p 11
31. Perdew JP, Chevary JA, Vosko SH, Jackson KA, Pederson MR, Singh DJ, Fiolhais C (1192) Phys Rev B 46:6671–6687
32. Perdew JP, Chevary JA, Vosko SH, Jackson KA, Pederson MR, Singh DJ, Fiolhais C (1993) Phys Rev B 48:4978
33. Perdew JP, Burke K, Wang Y (1996) Phys Rev B 54:16533–16539
34. Zhao Y, Schultz NE, Truhlar DG (2005) J Chem Phys 123: 161103
35. Zhao Y, Schultz NE, Truhlar DG (2006) J Chem Theor Comput 2:364–382
36. Zhao Y, Truhlar DG (2008) Theor Chem Acc 120:215–241
37. Cancès MT, Mennucci B, Tomasi J (1997) J Chem Phys 107:3032
38. Cossi M, Barone V, Mennucci B, Tomasi J (1998) Chem Phys Lett 286:253
39. Mennucci B, Tomasi J (1997) J Chem Phys 107:5151
40. Frisch MJ, Trucks GW, Schlegel HB, Scuseria GE, Robb MA, Cheeseman JR, Montgomery JA Jr, Vreven T, Kudin KN, Burant JC, Millam JM, Iyengar SS, Tomasi J, Barone V, Mennucci B, Cossi M, Scalmani G, Rega N, Petersson GA, Nakatsuji H, Hada M, Ehara M, Toyota K, Fukuda R, Hasegawa J, Ishida M, Nakajima T, Honda Y, Kitao O, Nakai H, Klene M, Li X, Knox JE, Hratchian HP, Cross JB, Adamo C, Jaramillo J, Gomperts R, Stratmann RE, Yazyev O, Austin AJ, Cammi R, Pomelli C, Ochterski JW, Ayala PY, Morokuma K, Voth GA, Salvador P, Dannenberg JJ, Zakrzewski VG, Dapprich S, Daniels AD, Strain MC, Farkas O, Malick DK, Rabuck AD, Raghavachari K, Foresman JB, Ortiz JV, Cui Q, Baboul AG, Clifford S, Cioslowski J, Stefanov BB, Liu G, Liashenko A, Piskorz P, Komaromi I, Martin RL, Fox DJ, Keith T, Al-Laham MA, Peng CY, Nanayakkara A, Challacombe M, Gill PMW, Johnson B, Chen W, Wong MW, Gonzalez C, Pople JA (2003) Gaussian 03(Revision E.01). Gaussian Inc., Pittsburgh
41. Lennard-Jones JE (1931) Proc Camb Phil Soc 27:469